SURMOF Devices Based on Heteroepitaxial Architectures with White-Light Emission and Luminescent Thermal-Dependent Performance

Dong-Hui Chen, Alexander E. Sedykh, Germán E. Gomez,* Beatrice Lilli Neumeier, Jaciara C. C. Santos, Vasily Gvilava, Ruben Maile, Claus Feldmann, Christof Wöll, Christoph Janiak, Klaus Müller-Buschbaum, and Engelbert Redel*

A new set of Ln-MOF (lanthanide-metal-organic framework) thin films, known as Ln-SURMOFs (surface-supported MOFs), is fabricated with a layer-by-layer, in order to generate solid-state white-lighting devices. A three-component approach is carried out for a rational combination of red, green, and blue (RGB) emitting Eu^{3+}, Tb^{3+}, and Gd^{3+} containing layers in order to achieve white-light emission. The Ln-SURMOFs are fully characterized by powder X-ray diffraction, infrared reflection–absorption spectroscopy, scanning electron microscopy, and photoluminescence spectroscopy (excitation-emission and chromaticity determination according to Commission International de l'Eclairage, CIE). The devices show CIE x,y coordinates of almost ideal white light (0.331, 0.329), as well as a correlated color temperature of 5570 K. Besides, the temperature dependent performance of the RGB-SURMOFs is studied at room temperature and at 77 K.

D.-H. Chen, Dr. J. C. C. Santos, V. Gvilava, Prof. C. Wöll, Dr. E. Redel
Institute of Functional Interfaces (IFG)
Karlsruhe Institute of Technology (KIT)
Hermann-von-Helmholtz-Platz 1
76344 Eggenstein-Leopoldshafen, Germany
E-mail: engelbert.redel@kit.edu

A. E. Sedykh, R. Maile, Prof. K. Müller-Buschbaum
Institut für Anorganische und Analytische Chemie
Justus-Liebig-Universität Gießen
Heinrich-Buff-Ring 17, 35392 Gießen, Germany

Dr. G. E. Gomez
Instituto de Investigaciones en Tecnología Química (INTEQUI)
Almirante Brown 1455, San Luis 5700, Argentina
E-mail: gegomez@unsl.edu.ar

Dr. B. L. Neumeier, Prof. C. Feldmann
Institut für Anorganische Chemie
Karlsruhe Institute of Technology (KIT)
Engesserstraße 15, D-76131 Karlsruhe, Germany

V. Gvilava, Prof. C. Janiak
Institut für Anorganische Chemie und Strukturchemie
Heinrich-Heine-Universität Düsseldorf
40225 Düsseldorf, Germany

Prof. K.-Müller-Buschbaum
Center for Materials Research (LaMa)
Justus-Liebig-Universität Gießen
Heinrich-Buff-Ring 16, 35392 Gießen, Germany

The prolific topic of development of solid-state lighting devices has focused over the last years on solid-state white light (SSWL) emitting materials, mainly due the long operation lifetime and excellent harvesting and saving energy.[1] Even today, incandescent and mercury-based fluorescent materials are employed as white-light sources due to their superior warm-white light impression. Moreover, the fabrication of environmentally safe white light-emitting diode (LEDs) with a "warm-white" impression remains still a challenge. Many of the "white" organic light-emitting diode/LED materials cover only part of the visible spectrum and lack the required efficacy of 150–200 lm W^{-1} for white-light performance.[2] For this reason, the design of a new generation of SSWL materials is of continuous interest in materials science, especially in areas such as full-color flat-panel electroluminescent displays for mobile devices, optical telecommunications, lighting, and back-lighting for liquid-crystals displays.[3]

Besides, high-quality white-light performance requires the Commission International de l'Eclairage (CIE) x,y coordinates 0.333, 0.333, with a correlated color temperature (CCT) into the 2500–6500 K, and color rendering index above 80 which are standard requirements for lighting applications.[4] One of the explored strategies to obtain white light is by combining red, green, and blue (RGB) sources to cover the visible region (400–700 nm) in the electromagnetic spectrum.[5]

Also, metal–organic frameworks (MOFs) have been the focus of interest due to their potential applications in gas storage/separation,[6] catalysis,[7] optics,[8] magnetism,[9] sensing,[10] and biomedicine.[4,11,12] Due to a permanent porosity, structural diversity, functionalization capabilities and then, tunable luminescence, MOF possess interesting properties for the development of SSWL composites. In recent years, a large number of luminescent MOFs have been reported for this purpose.[5,13–24] Moreover, for uses in nanotechnology, it is mandatory that MOFs are anchored on solid substrates, being particularly evident in the case of optoelectronic applications.[25,26] According to specialized reviews such as those from Wöll group,[27] it is distinguishable the surface-supported metal–organic frameworks (SURMOFs) devices, fabricated using layer-by-layer (LbL)

methodologies, where the orientation and film thickness can be well-controlled.

Besides, lanthanides are special in photonics due their optical features such as narrow bandwidth signal, pure color emission accompanied by a variety of lifetimes values.[28] However, Ln^{3+} ions have intrinsically low absorption coefficients, which need to be improved, e.g., by using aromatic ligands as light antenna to promote lanthanide phosphorescence.[29–31] Particularly, lanthanide-based MOFs (Ln-MOFs) have been widely explored to get highly pure white-light emission. This is achieved by the possibility of color emission modulation by doping different Ln^{3+} elements and by modulation of physical parameters such as excitation wavelength[13] and temperature.[32] For example, by a rational combination of the blue, red, and green emission colors white-light emission was achieved with Ln^{3+} intercalated into the pore system, for example, the MOFs[24,33] Eu^{3+},Tb^{3+}@ZJU-1 or Eu/Tb@IFP-1 and IFP-6 with CIE coordinates close to ideal white light,[24,33] among others.[15,17] Also, another strategy to produce SSWL devices is the incorporation of lanthanide-coordination compounds into HKUST-1 films.[34]

There are several methods for obtaining MOF thin films: either by deposition of presynthesized micropowder MOFs on the substrate, or by growing the MOF directly on the substrate.[27a] From the latter, the LbL method provides the advantage of controlling the thickness and morphology of the thin films, as linker and metal ion are introduced in cycles after one another.[27] Additionally, the liquid phase epitaxial method allows a deposition of hetero-multilayers.[27b] By constructing SURMOFs, it is possible to anchor MOFs onto functionalized solid substrates in a relatively easy manner by layer-by-layer methodologies, in spite of the high solvent consume and time required. At the end of this approach, thin-film systems are achieved, with the option to attain tunable properties, as the light emission can be modulated by controlling the number of different layers. Another advantage of SURMOFs is that a monolithic structure is formed, for which scattering effects are absent that are normal for powder-based MOFs (including thin-films produced from powder material), which may become crucial for some optical applications, generally when the substrate transparency is required, for example, for the transient optical absorption spectroscopy.[26]

Since lanthanide ions have similar ionic radii, it is possible to dope Ln-MOFs to tune a desired emission color using solvothermal methods.[35,36] Yet, the precursor concentration of the metal ions is not necessarily maintained as desired in the product. In addition, the energy transfer between two lanthanide ions additionally affects the color of the light emitted by the MOF. It would therefore be desirable to control the distance between different Ln ions, which are not possible for bulk MOFs fabricated using conventional methods.

The nanofabrication of the first set of Ln-SURMOF devices based on ordered crystals with controllable film thickness on transparent quartz substrates has recently been reported.[37] Therefore, thin-film processing of epitaxial grown Ln-SURMOFs can overcome concentration quenching in the bulk phase and provide a better color tuning.[37] To address the above challenges found in bulk crystals, the authors have applied an liquid phase epitaxy (LPE) process[38] for the thin film synthesis in an LbL fashion. By this methodology monolithic and transparent

SURMOFs were deposited on substrates with precise control of the film thickness.[39] Furthermore, it was reported that heteroepitaxial MOF growth on large crystal domains increases luminescence and provides a more controlled color tunability.[40,41]

In this work, the archetype MOF Ln(BTC) (BTC^{3-} = 1,3,5-benzenetricarboxylate) or MOF-76[42,43] was selected as basic structure to develop a multilayer SSWL emitting device. A three-component approach was selected to build single, double, and triple-layer devices in a sequential synthesis scheme. The high optical quality multilayer SURMOFs were deposited on transparent quartz substrates by an LbL method at 55 °C. By controlling the number of RGB layers, it was possible to achieve white-light emission. Also, the SSWL device was studied under diverse excitation wavelength at room temperature and 77 K, evidencing thermal-dependent behavior.

In MOF-76 each lanthanide ion is surrounded by six oxygen atoms from BTC and one oxygen atom from a terminal water molecule. The metal polyhedra are combined into helical chains along the c-axis, which are linked by the BTC ligands along the a- and b-axis giving rise to a 3D framework.[27b] The structure contains 1D solvent-filled channels running along the c-direction, with a circular cross-section of 36 $Å^2$. Previously, MOF-76 phase was obtained by the conventional solvothermal synthesis.[42,43] The first example of MOF-76 grown by LPE was recently reported, being an excellent approach to obtain an ordered crystalline SURMOF.[37] Over the last two decades, Wöll and colleagues have implemented the LPE technique for building SURMOFs for many applications, employing conventional MOFs such as ZIFs, IRMOF-n, MIL-n or HKUST-1, and recently UiO-NH_2-66.[27,44,45] Briefly, a pretreated quartz or silicon substrate was placed in a reactor at 55 °C (which is 10 °C lower than in our previous report).[37] Thereafter, the substrate was immersed in ethanolic solution of either $Ln(NO_3)_3$ or H_3BTC alternately. Between each immersion the substrate was rinsed thoroughly with pure ethanol, as described before.[27b] This process yielded optically transparent films of Ln-SURMOF. A detailed description of the SURMOF fabrication can be found in the Experimental Section. With this LPE technique, single, double and triple-layers systems were prepared.

Implementation of the LbL method allowed us to get a formation of thin MOF films with a defined thickness of individual Tb-, Gd-, and Eu-BTC layers in heteroepitaxial double- and triple-layer Ln-SURMOF (**Figure 1**a). By varying the thickness of each individual trivalent lanthanide layer, it is possible to tune the final emission color in a straightforward manner by changing the number of deposition cycles of each component. In order to fabricate heteroepitaxial architecture, we first deposited Tb-BTC SURMOF on the substrate followed by Eu-BTC in the middle and finally Gd-BTC of variable thickness on top.

The similar growth effect has been studied on HKUST-1 ($Cu_3(1,3,5-BTC)_2$) thin films by using a substrate functionalized with −COOH or −OH groups.[27b] The carboxylic acid groups can coordinate the Cu^{2+} ions, leading to a standup paddle wheel orientation, whereas employing hydroxyl groups leads to a parallel to the substrate orientation of the paddle wheel units.[27b] The latter is observed for Ln-BTC SURMOFs, where all the inorganic chains are oriented parallel to the substrate.

The in-plane powder X-ray diffraction profiles of Ln-SURMOFs reveal the presence of a unique phase constituted by
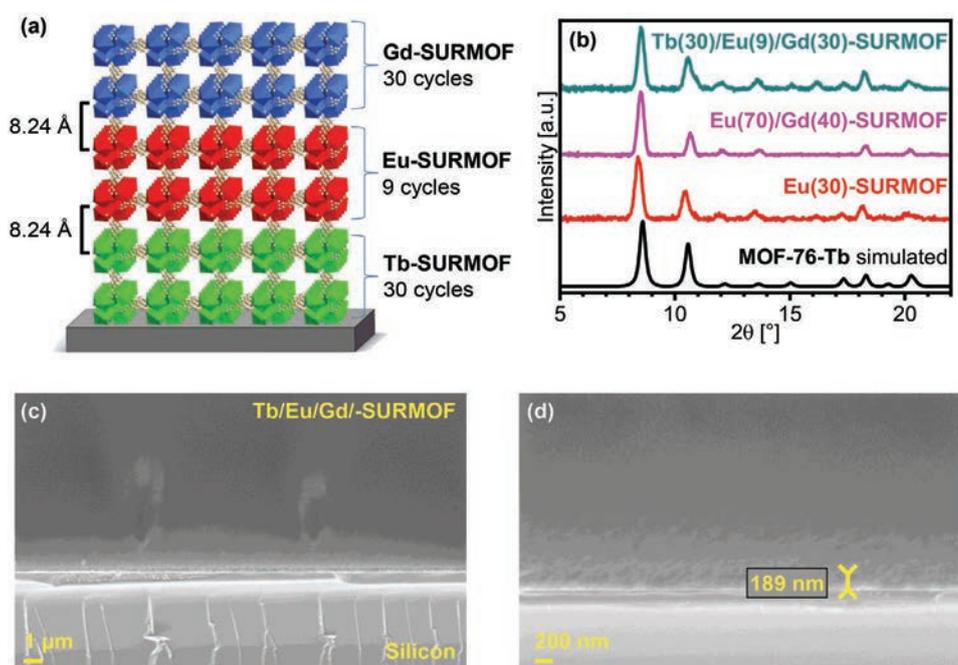
Figure 1. a) Scheme of the SURMOF device composed by RGB layers. b) The in-plane XRD profiles of the single, double and triple layers-SURMOFs. c,d) SEM images of the cross-section of Tb/Eu/Gd-SURMOF.

MOF-76 (Figure 1b). The out-of-plane X-ray diffraction data of the set of SURMOFs reported herein reveal the presence of highly crystalline, oriented films with a sharp diffraction peak at 8.52° (Figure S1, Supporting Information). This data shows an oriented growth of the MOF thin films along the [010] direction, with 1D channels oriented parallel to the substrate, as is it explained in our previous contribution.[40] For comparison, results from powder X-ray diffraction of the separate bulk Ln-BTC MOFs for Eu, Gd, Tb are shown in Figure S2 of the Supporting Information.

The vibrational analysis by infrared reflection absorption spectroscopy (IRRAS) was performed on SURMOFs onto SAM@Au substrates, (SAM, self-assembled monolayer). The IRRAS spectrum of Gd-SURMOF (Figure S3, Supporting Information) shows the asymmetric (1634 and 1540 cm^{-1}) and symmetric (1445 and 1406 cm^{-1}) vibrational transition modes of the COO– groups. Also, the absence of acidic OH bands supports the fact that the SURMOF was successfully grown and no residual linker was deposited in the film. Similar features were found in the IRRAS spectrum of the triple-layer system Tb/Eu/Gd-SURMOF, for which higher intense bands were observed compared to the Gd-SURMOF.

Moreover, the thickness and the roughness were also be studied from the images of the triple-layer SURMOFs by scanning electron microscope (SEM) measurements yielding a regular thickness of 190 nm, see Figure 1c,d.

Additionally, energy-dispersive X-ray spectroscopy analysis was performed including an area resolved mapping for Tb/Eu-SURMOF (Figure S4, Supporting Information) and Tb/Eu/Gd-SURMOF (Figure S5, Supporting Information). A uniform distribution of corresponding trivalent lanthanides was observed, however, individual layers could not be distinguished due to the low thickness of the films and resolution of the instrument.

ICP and XPS characterizations were also conducted; they were focused on the RGB-SURMOF, since it is the most promising material for the application reported in this work. The exact ratio of the lanthanide ions in RGB-SURMOF was determined by inductively coupled plasma optical emission spectrometry (ICP-OES) measurements, giving a constitution of $Tb_{0.31179}Eu_{0.1099}Gd_{0.5782}$-SURMOF. XPS analysis carried out on RGB-SURMOF provided information regarding the superficial features of the prepared device. According to the spectra shown in Figure S6 of the Supporting Information, higher intensity signals are attributed to Gd^{3+} ions ($3d_{3/2}$ and $3d_{5/2}$), C and O from the BTC^{3-} ligand. Lower intensity peaks are ascribed to Tb^{3+} and Eu^{3+} ions. This study also confirms in a semiquantitative way the amount of Gd^{3+} on top in comparison to the other lanthanides below.

According to the implemented strategy, a three-component system is required to promote white-light emission according to the RGB concept. First, the single-layer devices based solely on Tb, Eu, and Gd-SURMOFs were synthesized and optically characterized.

For the selection of a convenient blue-emitting layer, several Ln-SURMOFs with Ln = Ce, Pr, Gd, and Tm) were evaluated. Their emission spectra show the typical broad band of the BTC ligand belonging to $\pi^* \rightarrow \pi / n^* \rightarrow \pi$ aromatic ring transitions (Figure S7, Supporting Information).[46] For a blue-emitting layer, we decided to choose the Gd-SURMOF as its emission intensity was brighter than of other samples considered for a blue-emitting layer (Ln-SURMOFs with Ln = Ce, Pr, Tm), and additionally implementing Gd^{3+} in the structure of a Eu^{3+} or Tb^{3+} MOF increases the population of linker triplet states, which leads to 4f–4f Ln^{3+} emission of higher intensity.[47] In addition, an attempt employing Gd(SO$_3$CF$_3$)$_3$ as starting salt was carried out to avoid potential quenching by residual nitrate
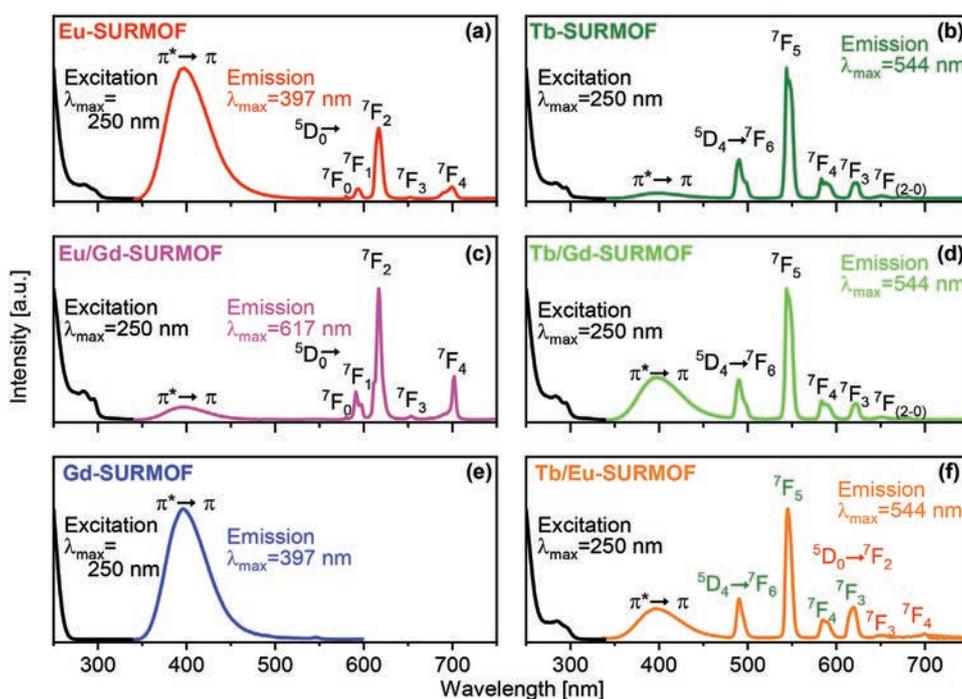
Figure 2. Normalized excitation and emission spectra of a,b,e) the single and c,d,f) double layers of Ln-SURMOFs. Recorded excitation spectra by monitoring the emissions at 617 nm for Eu- and Eu/Gd-SURMOF, 544 nm for Tb-, Tb/Gd-, and Tb/Eu-SURMOF, and 400 nm for Gd-SURMOF. The emission spectra were recorded at excitation wavelength of 255 nm.

groups. However, this resulted in a shift of the chromaticity from blue to cyan (see Figure S8, Supporting Information).

For monitoring the emission of the Eu-SURMOF at 617 nm, the excitation spectrum exhibits a broadband shoulder at 250 nm ascribed to $\pi^*\leftarrow\pi/\pi^*\leftarrow n$ ligand based transitions. Eu-SURMOF exhibits a magenta-colored emission consisting of the ligand $\pi^*\rightarrow\pi/n^*\rightarrow\pi$ transitions and the typical for Eu^{3+} $^5D_0\rightarrow^7F_J$ (J = 0-4) transitions with $^5D_0\rightarrow^7F_2$ as the highest intensity located at 617 nm (**Figure 2**a). High-relative intensity of the linker-based emission indicates a nonefficient energy transfer process from the excited states of the ligand to Eu^{3+} ions. For Tb-SURMOF, under the same excitation wavelength, a bright green emission was obtained, characterized by a fine structure in the spectrum belonging to the Tb^{3+} transitions of $^5D_4\rightarrow^7F_J$ (J = 6-1) with $^5D_4\rightarrow^7F_5$ at 544 nm being the most intense one (Figure 2b). For Tb-SURMOF, the ligand emission has lower relative intensity than 4f emission of the Tb^{3+}, indicating a more efficient energy transfer from ligand to metal.

For Eu/Gd-SURMOF, the ratio of Eu^{3+} 4f–4f emission to ligand-based emission is higher than for Eu-SURMOF (Figure 2a,c), as Gd in its layer is promoting the population of the triplet state[47] with the energy being transferred to the other layer containing Eu^{3+}. By contrast, for Tb/Gd-SURMOF, the relative intensity of the organic-based emission is higher than for a monolayer Tb sample (Figure 2b,d), which indicates that for Tb-SURMOF the energy transition from linkers to Tb^{3+} is already efficient. This corroborates the findings of the single-layer SURMOFs.

For an excitation at λ_{exc} = 255 nm, the emission spectrum of the double-layer Tb/Eu-SURMOF exhibits two sets of 4f–4f transitions belonging to Tb^{3+} and Eu^{3+} ions, as well as organic-based

emission, yielding a greenish-yellow color (Figure 2f). The Tb^{3+} transitions correspond to $^5D_4\rightarrow^7F_J$ (J = 6-4) with the $^5D_4\rightarrow^7F_5$ transition at 544 nm as the most intense one. The Eu^{3+} transitions $^5D_0\rightarrow^7F_J$ (J = 2-4) have $^5D_0\rightarrow^7F_2$ as the highest intense one located at 617 nm.

In the current literature of luminescent Ln-MOFs, the energy-transfer process between Tb^{3+} to Eu^{3+} ions is widely studied with the purpose to tune the resulting emission.[48–52] For this reason, a suitable distance between both centers is critical to promote or suppress this energy transfer. As previously demonstrated,[37] by an epitaxial SURMOF fabrication process, it is possible to control the energy transfer by exact position of each lanthanide-MOF in each layer of the interface region. By the LbL approach, it is now possible to tune chromaticity of the emission to a specific final color by changing the number of emitting layers. As discussed above, white-light emission can be achieved by a combination of three color-emitting layers. So, by a correct combination of red (Eu), green (Tb), and blue (Gd) emitting layers it is possible to generate white-light emission by designing an RGB-SURMOF.

Experimentally, the first Tb-SURMOF layer was anchored at the quartz substrate, then the Eu-SURMOF was grown as the middle layer and finally the Gd-SURMOF as the top layer. By varying the number of the deposition cycles for the Eu-, Tb-, and Gd-SURMOF layers, a more defined color can be achieved. However, also influences of metal exchange and inhomogeneity may result (Figure S9, Supporting Information). It was already reported that the separating distance between the adjacent MOF-76 SURMOF layers of 8.24 Å[37] is enough to avoid concentration quenching, which commonly occurs in Eu/Tb-codoped powder bulk systems.[53] Furthermore, by utilizing
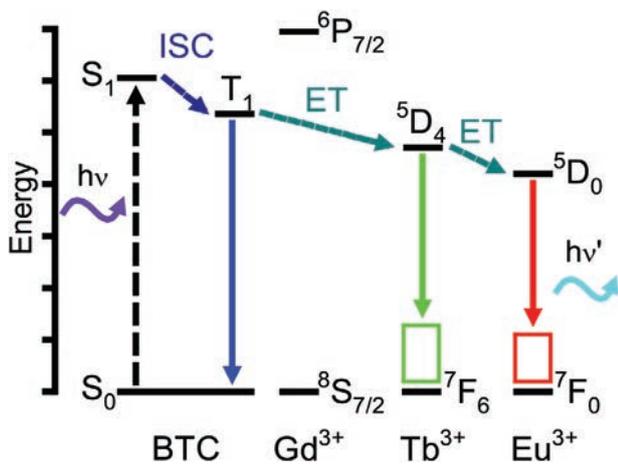
Figure 3. Proposed energy diagram of the Tb/Eu/Gd-SURMOF heteroepitaxial RGB architecture under UV excitation to yield SSWL.

the interface in heteroepitaxial Ln-SURMOF architectures,[37] a downshift from blue to red can be observed based on a metal–metal energy transfer process. Due to the higher position of the emitting levels for Tb^{3+} compared to Eu^{3+} (**Figure 3**), a "Dexter-type" energy migration from $Tb^{3+} \rightarrow Eu^{3+}$ is feasible with a distance of 8.24 Å between two Ln-SURMOF layers.

Excitation of Ln-SURMOFs architectures have been applied at different wavelengths. Since the spectra exhibit excitation depending maxima, this also leads to a variation of the resulting chromaticity, as ascribed in **Figure 4** and Figure S11 (Supporting Information). Even for different excitation, the RGB-SURMOF shows CCT values of 5570 K (λ_{exc} = 360 nm) and 3980 K (λ_{exc} = 320 nm) matching the human eye-friendly application range.[5]

As described before, Tb^{3+} and Eu^{3+} centered transitions were observed and dominate the single- and double-layer Tb/Eu-SURMOFs. In the triple-layer setting, both hypersensitive transitions exhibit higher intensities in comparison to the double and single layered Ln-SURMOFs, which is a condition to yield white-light emission in MOF systems.[54]

Upon excitation at 360 nm, the emission spectrum of the triple-layer Tb/Eu/Gd-SURMOF exhibits almost ideal white emission, showing CIE x,y coordinates of 0.331, 0.329 corresponding to the center of the CIE diagram (see Figure 4c) and representing a real RGB-SURMOF architecture. The corresponding values for a perfect white-light emitter are (0.333, 0.333) accompanied with a CCT of 5613 K.

In addition, the white-light performance of RGB-SURMOF can be compared to other white-light emitters in terms of CIE x,y chromaticities and CCT values. In the literature, luminescent MOFs play an important role for white-light emission with a significant number of examples of white-light emitters for powdered/bulk MOFs that exhibit emission of white light or close to the white point (for more information, see Table S1, Supporting Information).[13–24] However the implementation of thin films and eventually SURMOFs is scarcely reported.

The principal advantages of employing SURMOFs as white emitters can be summarized by the following aspects: device fabrication of diverse substrates, leading to desired chromaticity control by modulating the number of layers, and the possibility of constructing open structures to allow for host–guest interactions for multifunctional applications.

The obtained Ln-SURMOF emission chromaticity may not only depend on the constitution (see Figure S9 of the Supporting Information for the example of Tb/Eu/Gd-SURMOFs with different ratios of individual Ln^{3+} layers or homogeneity) as well as excitation wavelength (in addition, see Figure S10 of

Figure 4. Deliberate generation of white-light emission: a) excitation and emission spectra of the white emitting RGB architecture of Tb/Eu/Gd-SURMOF (the excitation spectrum was recorded by monitoring the emissions at 617 nm. The corresponding emission spectra were recorded at excitation wavelengths of 320 and 360 nm). b) Fabricated SURMOFs reported in the present work. c) CIE color coordinates x,y and a chromaticity diagram according to CIE of the optical devices presented and discussed in this work.

the Supporting Information with CIE color points for Ln-SUR-MOFs studied), but also on the temperature.

In order to study the responsive character of the reported set of materials, room and low temperature (RT and 77 K, respectively) measurements were carried out for all luminescent RGB Ln-SURMOF architectures. Upon cooling, the Ln^{3+} based 4f-4f emission of single-, double-, and triple-layer SURMOFs in spectra measured for an excitation of 255 nm increases in correspondence to the linker-based emission (Figures S12–S17, Supporting Information). This indicates a higher ligand triplet state population upon cooling and a better energy transition from the excited linker to lanthanide ions.[47] Besides, more fine structured 4f–4f transitions are observed in all the spectra if recorded at 77 K due to a reduction of thermal quenching.[48] Under excitation with UV-light of either 320 or 360 nm wavelength, ligand-based emission relative intensity of the triple-layer Ln-SURMOF rises upon cooling (Figure S18, Supporting Information). All these spectroscopic features produce shifts in the CIE color diagram, leading to different responses according to the excitation wavelength for RT and 77 K (Figure S10, Supporting Information).

New Ln-SURMOFs based on MOF-76 crystalline architecture were obtained for solid-state lighting employing an LbL approach. By this technique, homogenous devices of 200 nm of thickness were obtained. Thereby, a deliberate design for solid-state white lighting (SSWL) performance was achieved by multiple emitting layers and the addition of three colors according to the RGB concept (red, green, and blue). The Tb/Eu/Gd-SURMOF RGB device shows CIE x,y coordinates close to ideal for white light (0.331, 0.329) upon excitation at 360 nm. Also, the CCT was evaluated as human-eye friendly for potential applications, giving 5614 and 4411 K values, corresponding to SSWL performances. Besides, the luminescence of all the SUR-MOFs was evaluated at room and low temperature (77 K) giving rise to options for different color performance depending on temperature and excitation energy, being a "key" property for the design of thermal-sensor in cryogenic ranges. Finally, control of thickness, homogeneity, and emission color has been reached by employing the heteroepitaxial approach using lanthanide MOF architectures.

Experimental Section

Fabrication of Single-Layer SURMOFs: Fabrication of single-layer Ln-SURMOFs (Ln = Pr, Eu, Gd, Tb, Tm). Quartz substrates were cleaned by immersing in ethanol and sonicating for 30 min. Then the quartz substrates were dried in a stream of N_2 gas and were treated by oxygen plasma for 30 min to remove impurities and increase the number of OH functional groups. Ln-SURMOFs were grown on the treated quartz substrates by liquid-phase epitaxy at 55 °C. First the substrates were immersed into a 4×10^{-4} mol L^{-1} ethanolic solution of $Ln(NO_3)_3$ for 12 min. After rinsing with pure ethanol, the quartz substrates were immersed in 1×10^{-3} mol L^{-1} ethanolic solution of H_3BTC for 12 min. Then the quartz substrates were rinsed by pure ethanol again. The growth process was repeated over 70 cycles.

Fabrication of Double-Layer Ln/Ln′-SURMOFs: The first layer was grown as described before for the single-layer Ln-SURMOF. After having repeated the growth process for the first layer over the set number of cycles, the same procedure was carried out in order to grow the second layer. By this process, double layers of Eu/Gd-SURMOF (70/40 cycles),

Tb/Gd-SURMOF (30/20 cycles), Tb/Eu-SURMOF (30/4 cycles), and Eu/Tb-SURMOF (70/70 cycles) were obtained.

Fabrication of the Triple-Layer Tb/Eu/Gd-SURMOF: The first step was the fabrication of Tb-SURMOF on the quartz substrates using the previous procedure for the single-layer Ln-SURMOF. After a constant number of 30 cycles of LbL growth process, the substrates were immersed into 4×10^{-4} mol L^{-1} ethanolic solution of $Eu(NO_3)_3$ for 12 min and rinsed with pure ethanol. In the next step, the quartz substrates were immersed in 1×10^{-3} mol L^{-1} ethanolic solution of H_3BTC for 12 min and rinsed with pure ethanol again. The Eu-SURMOF LbL-growth process was repeated from 4 to 9 cycles. Finally, the Gd-SURMOF layer was grown on top of the device employing the same conditions as for the Eu and Tb-layers. For Gd, 30 layers were deposited.

Synthesis of Bulk Ln-BTC MOFs: $[Gd(BTC)(H_2O)]\cdot(DMF)$ $(H_2O)_{0.5}(1\text{-}H_2O\cdot DMF)$ was synthesized according to the literature.[55] $GdCl_3\cdot6H_2O$ (0.192 g, 0.5 mmol) and H_3BTC (0.128 g, 0.6 mmol) were dissolved in 9 mL of DMF and 3 mL of deionized water. Then the reaction mixture was placed in a 24 mL Teflon-lined reactor. The reactor was sealed and heated at 80 °C for 72 h. The colorless crystals were collected by filtrating, washed with DMF and dried under vacuum.

$[Ce(BTC)(H_2O)]\cdot(DMF)_n$ was synthesized according to the literature.[56] $Ce(NO_3)_3\cdot6H_2O$ (0.083 g, 0.190 mmol) and H_3BTC (0.083 g, 0.381 mmol) were dissolved in 16 mL of DMF. Then the reaction mixture was placed in a 24 mL Teflon-lined reactor. The reactor was sealed and heated at 80 °C for 64 h. The colorless crystals were collected by filtrating, washed with DMF and ethanol and dried under vacuum.

$[Eu(BTC)(H_2O)]$ was synthesized according to the literature.[57] $Eu(NO_3)_3\cdot6H_2O$ (0.045 g, 0.10 mmol) and H_3BTC (0.021 g, 0.10 mmol) were dissolved in 10 mL of DMF, 2 mL of deionized water, 2 mL of cyclohexanol, and 2 drops of dibutylamine. Drops of nitric acid were added to reach a pH of 5. The reaction mixture was stirred 2 h at room temperature and then heated under reflux for 17 h at 85 °C. The colorless crystals were collected by filtrating, washed with DMF and methanol, and dried under vacuum.

$[Tb(BTC)(H_2O)_{1.5}]\cdot(DMF)$ was synthesized according to the literature.[58] $Tb(NO_3)_3\cdot6H_2O$ (0.123 g, 0.272 mmol) and H_3BTC (0.021 g, 0.10 mmol) were dissolved in 4 mL of DMF, 4 mL of ethanol, and 3.2 mL of deionized water. Then the reaction mixture was placed in a 24 mL Teflon-lined reactor. The reactor was sealed and heated at 80 °C for 24 h. The colorless crystals were collected by filtrating, washed with ethanol, and dried under vacuum.

Keywords

[1] E. F. Schubert, J. K. Kim, *Science* **2005**, *308*, 1274.

[2] Y. Narukawa, M. Ichikawa, D. Sanga, M. Sano, T. Mukai, *J. Phys. D: Appl. Phys.* **2010**, *43*, 354002.

[3] a) S. Choi, Y. J. Yun, H.-K. Jung, *Mater. Lett.* **2012**, *75*, 186; b) A. C. Grimsdale, K. Leok Chan, R. E. Martin, P. G. Jokisz, A. B. Holmes, *Chem. Rev.* **2009**, *109*, 897; c) H. Liu, F. Liu, P. Lu, *J. Mater. Chem. C* **2020**, *8*, 5636.

[4] a) Y. S. Zhao, H. Fu, F. Hu, A. Peng, W. Yang, J. Yao, *Adv. Mater.* **2008**, *20*, 79; b) N. Willis-Fox, M. Kraft, J. Arlt, U. Scherf, R. C. Evans, *Adv. Funct. Mater.* **2016**, *26*, 532; c) E. R. Dohner, E. T. Hoke, H. I. Karunadasa, *J. Am. Chem. Soc.* **2014**, *136*, 1718.

[5] S. S. Lekshmi, A. R. Ramya, M. L. P. Reddy, S. Varughese, *J. Photochem. Photobiol., C* **2017**, *33*, 109.

[6] a) R. B. Getman, Y.-S. Bae, C. E. Wilmer, R. Q. Snurr, *Chem. Rev.* **2012**, *112*, 703; b) K. Adil, Y. Belmabkhout, R. S. Pillai, A. Cadiau, P. M. Bhatt, A. H. Assen, G. Maurin, M. Eddaoudi, *Chem. Soc. Rev.* **2017**, *46*, 3402.

[7] a) J. D. Evans, B. Garai, H. Reinsch, W. Li, S. Dissegna, V. Bon, I. Senkovska, R. A. Fischer, S. Kaskel, C. Janiak, N. Stock, D. Volkmer, *Coord. Chem. Rev.* **2019**, *380*, 378; b) S. M. J. Rogge, A. Bavykina, J. Hajek, H. Garcia, A. I. Olivos-Suarez, A. Sepúlveda-Escribano, A. Vimont, G. Clet, P. Bazin, F. Kapteijn, M. Daturi, E. V. Ramos-Fernandez, F. X. Llabrés i Xamena, V. Van Speybroeck, J. Gascon, *Chem. Soc. Rev.* **2017**, *46*, 3134.

[8] a) R. Medishetty, J. K. Zareba, D. Mayer, M. Samoć, R. A. Fischer, *Chem. Soc. Rev.* **2017**, *46*, 4976; b) K. Müller-Buschbaum, F. Beuerle, C. Feldmann, *Microporous Mesoporous Mater.* **2015**, *216*, 171; c) B. Li, H.-M. Wen, Y. Cui, W. Zhou, G. Qian, B. Chen, *Adv. Mater.* **2016**, *28*, 8819; d) Z. Hu, B. J. Deibert, J. Li, *Chem. Soc. Rev.* **2014**, *43*, 5815.

[9] G. Mínguez Espallargas, E. Coronado, *Chem. Soc. Rev.* **2018**, *47*, 533.

[10] a) Y. M. Zhang, S. Yuan, G. Day, X. Wang, X. Y. Yang, H. C. Zhou, *Coord. Chem. Rev.* **2018**, *354*, 28; b) W. P. Lustig, S. Mukherjee, N. D. Rudd, A. V. Desai, J. Li, S. K. Ghosh, *Chem. Soc. Rev.* **2017**, *46*, 3242; c) L. V. Meyer, F. Schönfeld, K. Müller-Buschbaum, *Chem. Commun.* **2014**, *50*, 8093; d) J. M. Stangl, D. Dietrich, A. E. Sedykh, C. Janiak, K. Müller-Buschbaum, *J. Mater. Chem. C* **2018**, *6*, 9248.

[11] X. Lian, Y.u Fang, E. Joseph, Q. Wang, J. Li, S. Banerjee, C. Lollar, X. Wang, H.-C. Zhou, *Chem. Soc. Rev.* **2017**, *46*, 3386.

[12] G. Maurin, C. Serre, A. Cooper, G. Férey, *Chem. Soc. Rev.* **2017**, *46*, 3104.

[13] X. Rao, Q. Huang, X. Yang, Y. Cui, Y. Yang, C. Wu, B. Chen, G. Qian, *J. Mater. Chem.* **2012**, *22*, 3210.

[14] S. Dang, J.-H. Zhang, Z.-M. Sun, *J. Mater. Chem.* **2012**, *22*, 8868.

[15] N. Kerbellec, D. Kustaryono, V. Haquin, M. Etienne, C. Daiguebonne, O. Guillou, *Inorg. Chem.* **2009**, *48*, 2837.

[16] L. L. da Luz, B. F. Lucena Viana, G. C. O. da Silva, C. C. Gatto, A. M. Fontes, M. Malta, I. T. Weber, M. O. Rodrigues, A. Junior, *CrystEngComm* **2014**, *16*, 6914.

[17] X.-L. Qu, B. Yan, *Inorg. Chem.* **2018**, *57*, 7815.

[18] S.-M. Li, X.-J. Zheng, D.-Q. Yuan, A. Ablet, L.-P. Jin, *Inorg. Chem.* **2012**, *51*, 1201.

[19] M.-L. Ma, J.-H. Qin, C. Ji, H. Xu, R. Wang, B.-J. Li, S.-Q. Zang, H.-W. Hou, S. R.Batten, *J. Mater. Chem. C* **2014**, *2*, 1085.

[20] Z.-F. Liu, M.-F. Wu, S.-H. Wang, F.-K. Zheng, G.-E. Wang, J. Chen, Y. Xiao, A.-Q. Wu, G.-C. Guo, J.-S. Huang, *J. Mater. Chem. C* **2013**, *1*, 4634.

[21] X. Ma, X. Li, Y.-E. Cha, L.-P. Jin, *Cryst. Growth Des.* **2012**, *12*, 5227.

[22] B.-H. Wang, B. Yan, *J. Alloys Compd.* **2019**, *777*, 415.

[23] H. Liu, T. Chu, Z. Rao, S. Wang, Y. Yang, W.-T. Wong, *Adv. Opt. Mater.* **2015**, *3*, 1545.

[24] S. S. Mondal, K. Behrens, P. R. Matthes, F. Schönfeld, J. Nitzsch, A. Steffen, P.-A. Primus, M. U. Kumke, K. Müller-Buschbaum, H.-J. Holdt, *J. Mater. Chem. C* **2015**, *3*, 4623.

[25] M. D. Allendorf, A. Schwartzberg, V. Stavila, A. A. Talin, *Chem. - Eur. J.* **2011**, *17*, 11372.

[26] a) R. Haldar, L. Heinke, C. Wöll, *Adv. Mater.* **2019**, *32*, 1905227; b) Z.-G. Gu, A. Pfriem, S. Hamsch, H. Breitweiser, J. Wolkgemuth, L. Heinke, H. Gliemann, C. Wöll, *Microporous Mesoporous Mater.* **2015**, *211*, 82.

[27] a) J. Liu, C. Wöll, *Chem. Soc. Rev.* **2017**, *46*, 5730; b) Z. Wang, C. Wöll, *Adv. Mater. Technol.* **2019**, *4*, 1800413.

[28] J.-C. G. Bünzli, S. Comby, A.-S. Chauvin, C. D. B. Vandevyver, *J. Rare Earths* **2007**, *25*, 257.

[29] M. D. Allendorf, C. A. Bauer, R. K. Bhakta, R. J. Houk, *Chem. Soc. Rev.* **2009**, *38*, 1330.

[30] A. E. Sedykh, D. G. Kurth, K. Müller-Buschbaum, *Eur. J. Inorg. Chem.* **2019**, *2019*, 4564.

[31] G. E. Gomez, M. C. Bernini, E. V. Brusau, G. E. Narda, D. Vega, A. M. Kaczmarek, R. Van Deun, M. Nazzarro, *Dalton Trans.* **2015**, *44*, 3417.

[32] J. Rocha, C. D. S. Brites, L. D. Carlos, *Chem. - Eur. J.* **2016**, *22*, 14782.

[33] S. S. Mondal, A. Bhunia, A. G. Attallah, P. R. Matthes, A. Kelling, U. Schilde, K. Müller-Buschbaum, R. Krause-Rehberg, C. Janiak, H.-J. Holdt, *Chem. - Eur. J.* **2016**, *22*, 6905.

[34] Z.-G. Gu, Z. C., W.-Q. Fu, F. Wang, J. Zhang, *ACS Appl. Mater. Interfaces* **2015**, *7*, 28585.

[35] Y. Su, Y. Yu, Y. Li, S. F. Z. Phua, G. Liu, W. Q. Lim, X. Yang, R. Ganguly, C. Dang, C. Yang, Y. Zhao, *Commun. Chem.* **2018**, *1*, 12.

[36] G. E. Gomez, E. V. Brusau, A. M. Kaczmarek, C. Mellot-Draznieks, J. Sacanell, G. Rousse, R. V. Deun, C. Sanchez, G. E. Narda, G. J. A. A. Soler Illia, *Eur. J. Inorg. Chem.* **2017**, *2017*, 2321.

[37] D.-H. Chen, H. R, B. L. Neumeier, Z.-H. Fu, C. Feldmann, C. Wöll, E. Redel, *Adv. Funct. Mater.* **2019**, *29*, 1903086.

[38] S. Furukawa, K. Hirai, K. Nakagawa, Y. Takashima, R. Matsuda, T. Tsuruoka, M. Kondo, R. Haruki, D. Tanaka, H. Sakamoto, S. Shimomura, O. Sakata, S. Kitagawa, *Angew. Chem., Int. Ed.* **2009**, *48*, 1766.

[39] D. Zacher, K. Yusenko, A. Betard, S. Henke, M. Molon, T. Ladnorg, O. Shekhah, B. Schüpbach, T. de los Arcos, M. Krasnopolski, M. Meilikhov, J. Winter, A. Terfort, C. Wöll, R. A. Fischer, *Chem. - Eur. J.* **2011**, *17*, 1448.

[40] M. Pan, Y.-X. Zhu, K. Wu, L. Chen, Y.-J. Hou, S.-Y. Yin, H.-P. Wang, Y.-N. Fan, C.-Y. Su, *Angew. Chem., Int. Ed.* **2017**, *56*, 14582.

[41] L. L. da Luz, B. F. L. Viana, G. C. Oliveira da Silva, C. C. Gatto, A. M. Fontes, M. Malta, I. T. Weber, M. O. Rodrigues, S. A. Júnior, *CrystEngComm* **2014**, *16*, 6914.

[42] B. Chen, L. Wang, F. Zapata, G. Qian, E. B. Lobkovsky, *J. Am. Chem. Soc.* **2008**, *130*, 6718.

[43] G. E. Gomez, M. dos Santos Afonso, H. A. Baldoni, F. Roncaroli, G. J. A. A. Soler-Illia, *Sensors* **2019**, *19*, 1260.

[44] O. Shekhah, H. Wang, S. Kowarik, F. Schreiber, M. Paulus, M. Tolan, C. Sternemann, F. Evers, D. Zacher, R. A. Fischer, C. Wöll, *J. Am. Chem. Soc.* **2007**, *129*, 15118.

[45] T. Hashem, E. P. Valadez Sánchez, P. G. Weidler, H. Gliemann, M. H. Alkordi, C. Wöll, *ChemistryOpen* **2020**, *9*, 524.

[46] G. E. Gomez, A. M. Kaczmarek, R. Van Deun, E. V. Brusau, G. E. Narda, D. Vega, M. Iglesias, E. Gutierrez-Puebla, M. Ángeles Monge, *Eur. J. Inorg. Chem.* **2016**, *2016*, 1577.

[47] R. F. D'Vries, S. Alvarez-García, N. Snejko, L. E. Bausá, E. Gutiérrez-Puebla, A. de Andrés, M. Á. Monge, *J. Mater. Chem. C* **2013**, *1*, 6316.

[48] a) J. C. Zhang, C. Pan, Y. F. Zhu, L. Z. Zhao, H. W. He, X. F. Liu, J. R. Qiu, *Adv. Mater.* **2018**, *30*, 1804644; b) J.-F. Feng, S.-Y. Gao, T.-F. Liu, J. Shi, R. Cao, *ACS Appl. Mater. Interfaces* **2018**, *10*, 6014; c) J.-F. Feng, T.-F. Liu, J. Shi, S.-Y. Gao, R. Cao, *ACS Appl. Mater. Interfaces* **2018**, *10*, 20854; d) J.-F. Feng, X.-Y. Yan, Z.-Y. Ji, T.-F. Liu, R. Cao, *ACS Appl. Mater. Interfaces* **2020**, *12*, 29854.

[49] Y.-W. Zhao, F.-Q. Zhang, X.-M. Zhang, *ACS Appl. Mater. Interfaces* **2016**, *8*, 24123.

[50] S. Mohapatra, S. Adhikari, H. Riju, T. K. Maji, *Inorg. Chem.* **2012**, *51*, 4891.

[51] D. T. de Lill, A. de Bettencourt-Dias, C. L. Cahill, *Inorg. Chem.* **2007**, *46*, 3960.

[52] G. Makhloufi, B. Francis, J. Dechnik, A. Strzelczyk, C. Janiak, *Polyhedron* **2017**, *127*, 59.

[53] a) J. Heine, K. Müller-Buschbaum, *Chem. Soc. Rev.* **2013**, *42*, 9232; b) K. Binnemans, *Chem. Rev.* **2009**, *109*, 4283; c) D. Liu, K. Lu, C. Poon, W. Lin, *Inorg. Chem.* **2014**, *53*, 1916.

[54] C. Krishnaraj, A. M. Kaczmarek, H. S. Jena, K. Leus, N. Chaoui, J. Schmidt, R. Van Deun, P. Van Der Voort, *ACS Appl. Mater. Interfaces* **2019**, *11*, 27343.

[55] L. H. Xie, Y. Wang, X. M. Liu, J. Bin Lin, J. P. Zhang, X. M. Chen, *CrystEngComm* **2011**, *13*, 5849.

[56] M. Almáši, V. Zeleňák, M. Opanasenko, I. Císařová, *Catal. Today* **2015**, *243*, 184.

[57] M. Gustafsson, A. Bartoszewicz, B. Martiín-Matute, J. Sun, J. Grins, T. Zhao, Z. Li, G. Zhu, X. Zou, *Chem. Mater.* **2010**, *22*, 3316.

[58] N. L. Rosi, J. Kim, M. Eddaoudi, B. Chen, M. O'Keeffe, O. M. Yaghi, *J. Am. Chem. Soc.* **2005**, *127*, 1504.

Repository KITopen